



# Three novel copula-based bias correction methods for daily ECMWF air temperature data

Fakherreh Alidoost<sup>1</sup>, Alfred Stein<sup>1</sup>, Zhongbo Su<sup>1</sup>, Ali Sharifi<sup>1</sup>

<sup>1</sup>ITC, University of Twente, Enschede, 7500AE, the Netherlands

5 *Correspondence to:* Fakherreh Alidoost (f.alidoost@utwente.nl)

**Abstract.** Data retrieved from global weather forecast systems are typically biased with respect to measurements at local weather stations. This paper presents three copula-based methods for bias correction of daily air temperature data derived from the European Centre for Medium-range Weather Forecasts (ECMWF). The aim is to predict conditional copula quantiles at different unvisited locations, assuming spatial stationarity of the underlying random field. The three new methods are: bivariate  
10 copula quantile mapping (types I and II), and a quantile search. These are compared with commonly applied methods, using data from an agricultural area in the Qazvin Plain in Iran containing five weather stations. Cross-validation is carried out to assess the performance. The study shows that the new methods are able to predict the conditional quantiles at unvisited locations, improve the higher order moments of marginal distributions, and take the spatial variabilities of the bias-corrected variable into account. It further illustrates how a choice of the bias correction method affects the bias-corrected variable and  
15 highlights both theoretical and practical issues of the methods. We conclude that the three new methods improve local refinement of weather data, in particular if a low number of observations is available.

## 1 Introduction

Weather stations are often sparse and usually located at irregular positions. If their data are used for crop growth simulations, then their results at unvisited locations are likely to be uncertain. A solution to this problem is to use weather data from a  
20 weather forecast system at each location. A modern and reliable weather forecast system is commonly composed of dynamical models, data assimilation methods and a product delivery system (Persson 2013). The coarse resolution of models, mutual dependence of weather parameters, and variability of these parameters in space and time, however, result in system uncertainties of the obtained weather data (Dee et al. 2011; Durai and Bhradwaj 2014). The uncertainties propagate as they are further applied, e.g. in hydrological models that increasingly use such data as input. This requires the data to be corrected  
25 before being used.

Bias is defined as the systematic underestimation or overestimation of a global weather forecast system with respect to local measurements from weather stations (Persson 2013; Mao et al. 2015). Various bias correction methods have been proposed in the literature: linear-scaling factor methods (Lenderink et al. 2007), nonlinear methods (Lafon et al. 2013), and quantile mapping methods (Ines and Hansen 2006). These methods are able to correct for bias in the mean, but they do not consider



other moments of a probability distribution. Currently, the bivariate Gamma and empirical distributions are specifically used for bias correction of precipitation data and the Gaussian distribution for bias correction of temperature data. A limitation of this approach is that the same distributions families are used to estimate both the marginal and the multivariate distributions (Genest and Favre 2007). For this reason, we turn to copulas.

- 5 A copula joins a multivariate distribution to its univariate marginals, based upon Sklar's theorem (Sklar 1973; Nelsen 2006). Copulas describe the complex dependence structure between variables independently from the marginal distributions (Gräler and Pebesma 2011). Recently, copula-based methods have been developed for deriving bias-corrected weather data. Here, a conditional distribution describes the dependence structure between weather forecast data and measurements at weather stations. Their estimated quantiles are transformed into bias-corrected weather data.
- 10 A bias correction method proposed by Laux et al. (2011) employed a bivariate conditional copula distribution for the precipitation time series retrieved from a regional climate model. Mao et al. (2015) investigated daily precipitation data and showed that a copula-based bias correction performs better than quantile mapping. Vogl et al. (2012) proposed the "Multiple Theta" and the "Maximum Theta" approaches for bias correction of rainfall data. So far, copulas have mainly been applied to precipitation time series retrieved from regional climate models. Observed weather data, in contrast, are provided at various
- 15 temporal resolutions, whereas bias correction is often assumed to be temporally stationary. This means that they are also valid for future conditions (Teutschbein and Seibert 2012).

This paper presents three new methods based on the copula concept: bivariate copula quantile mapping (types I and II), and quantile search. The new methods allow for estimating different conditional quantiles at different unvisited locations for each time step of a time series. Another aim is to evaluate these methods to predict the spatial variability of the bias-corrected daily

- 20 air temperature at unvisited locations. In addition, this paper compares available bias correction methods, which are marginal quantile mapping, expectation predictor and single quantile predictor. The expectation and single quantile predictors are based on the bivariate conditional copula. The aim is to provide a review of these methods for bias correction of the daily air temperature data when relatively low number of observations are available.

The structure of this paper is as follows. The concept of copula and the methods of bias correction are presented in Sect. 2.

- 25 The study area and data are introduced in Sect. 3. The results of bias correction methods for the study area are described in Section 4, followed by the discussion and conclusion in Sect. 5 and Sect. 6.

## 2 Method

### 2.1 Copulas

- 30 A copula is a multivariate cumulative distribution function that describes the dependence structure between variables. This function is unique if the marginals are continuous functions (Nelsen 2006; Vogl et al. 2012). According to Sklar's theorem, the joint multivariate distribution  $H$  of  $m$  variables  $Z_i$  equals a copula  $C$  of  $m$  variables  $u_i$  as:

$$H(z_1, \dots, z_m) = C(u_1, \dots, u_m). \quad (1)$$



$$u_i = F_i(z_i), \quad u_i \in [0,1]. \quad (2)$$

where  $F_i$  is the marginal distribution function. A bivariate copula can describe several dependence structures: the spatial dependence structure between two variables at two different locations in space or at two different points in time; the spatio-temporal dependence structure between two variables at different points in time and space; the dependence structure between two variables at one point in time and space. A bivariate conditional copula  $C_{u_2}^t(u_1)$  is often used to correct for bias by describing the dependence structure between two variables at one point in time and space, where  $u_1$  is treated as “true” variable and  $u_2$  is biased variable. Several copula families have been developed to capture multivariate joint distributions such as the Gaussian, the Student’s  $t$ , the Clayton, the Gumbel and the Frank families (Nelsen 2006). These families mainly differ in the way the tail dependence structure is described (Table 1) (Joe 1993; Manner 2007).

## 2.2 Copula-based bias correction method

The bias at time  $t$  and location  $s$  is defined as the difference between the measurements from weather stations denoted by  $Z_1$ , and weather forecasts denoted by  $Z_2$ :

$$Z_1 = Z_2 + Bias. \quad (3)$$

The value of the bias is predicted indirectly in copula-based bias correction methods. A bivariate conditional copula  $C_{u_2}^t(u_1)$  for two variables at one point in space and time, denoted by  $Z_1$  and  $Z_2$ , is defined as (Nelsen 2006):

$$P(Z_1 \leq z_1 | Z_2 = z_2) = C_{u_2}^t(u_1) = C^t(u_1 | u_2) = \frac{\partial C^t(u_1, u_2)}{\partial u_2} = p_{u_1}, \quad C: [0,1]^2 \rightarrow [0,1]. \quad (4)$$

where  $u_1$  and  $u_2$  are empirical marginal quantiles. Throughout, the functions and variable vary over space and time;  $s$  refers to a location and  $t$  refers to single moment in time. We assumed spatial stationarity to estimate  $C^t$ . This assumption is justified as the dependence structure between the observed and the forecasted variables is studied in a relatively small area and the dependence structures are thus unlikely to change in a non-stationary way.

Empirical marginal distributions  $u_1$  and  $u_2$  are obtained using the following rank-order-transformation:

$$u_i = \frac{\text{rank}(Z_i)}{k+1}. \quad (5)$$

where  $k$  denotes the number of available data for  $Z_i$ . We denote the transformed variables by  $u_1$  and  $u_2$  for the conditioned and conditioning variables, which are now approximately uniformly distributed on  $[0, 1]$ . Extreme values that possibly exist in the observations, however, are smoothed and hence the extreme values cannot occur at unvisited locations after this transformation. To solve for this problem and to obtain a better approximation of the marginal distribution function at unvisited locations, a polynomial is fitted to the pairs  $(z_1, u_1)$ . Yet, this approach is also prone to uncertainty because the polynomial is fitted to a low number of observed values.

To further proceed, a bivariate copula is fitted to the marginal quantiles  $u_1$  and  $u_2$  at weather stations for each time step. We use the Student’s  $t$  (Demarta and McNeil 2005), Gaussian, the Clayton, the Gumbel and the Frank families (Joe 1993), as these families are sufficiently flexible to capture the dependence structures of the conditioned and conditioning variables pairs  $(u_1,$



$u_2$ ). Note that a bivariate copula has one parameter, except the Student's  $t$  family that has two parameters: one for the correlation and one for the degrees of freedom (Table 1). To estimate the parameters for each family, we apply maximum likelihood estimation, using starting values obtained by Kendall's  $\tau$ , being a measure of association between variables (Nelsen 2006). Based upon their results, the most suitable family is selected according to Akaike's Information Criteria (AIC) (Akaike 1974).

5 In copula-based bias correction methods, the conditional quantile  $p_{u_1}$  needs to be predicted to derive the marginal quantile  $\hat{u}_1$  as well as the realization of the random variable  $\hat{Z}_1$ . The solution depends upon the application, i.e.  $\hat{Z}_1$  has to be predicted at the unvisited location in space, at the unobserved period in time or both. Incorporating temporal/spatial information or spatio-temporal information of available data to predict the conditional quantile then likely affects selection of a suitable method.

## 10 2.3 Realization of random variable $\hat{Z}_1$

The purpose of the bias correction method is to predict the bias-corrected values at unvisited locations. This section describes briefly available methods to obtain the realizations of the bias-corrected variable  $\hat{Z}_1$  and compares them to the three newly developed methods.

### 2.3.1 Marginal quantile mapping

15 A comprehensive study carried out by Teutschbein and Seibert (2012) showed that the quantile mapping method performs best among the classical bias correction methods and it can easily be implemented. It can reduce bias in the first two moments of a probability distribution. It is, however, sensitive to the number of quantile divisions when using an empirical probability distribution. For this method, several names can be found in the literature, such as probability mapping, CDF matching, quantile-quantile mapping. Here, we call this method as marginal quantile mapping (MQM) to specify the type of cumulative  
 20 distribution function in the mapping and compare it to the copula-based bias correction methods. In the marginal quantile mapping, a single value  $\hat{z}_1$  as a realization of the random variable  $\hat{Z}_1$  is obtained as:

$$\hat{z}_1 = (F_1^t)^{-1}(F_2^t(z_2)). \quad (6)$$

The idea of MQM is that there is a perfect dependence between variables  $u_1$  and  $u_2$ . This underlying assumption, however, is hard to be fulfilled, due to the complexity of the dependence structure between measurements and forecasted data.

### 25 2.3.2 Expectation predictor

The conditional expectation is the optimal predictor, in the sense that it minimize the Bayes risk (Cressie 1993). It can be either linear or nonlinear in  $Z_1$ . A single value  $\hat{z}_{1(mean)}$  as a realization of the random variable  $\hat{Z}_1^{t,s}$  is obtained using the conditional expectation (Bárdossy and Li 2008):

$$\hat{z}_{1(mean)} = E[z_1 | z_2] = \int_{z_1} z_1 \cdot f^t(Z_1 | Z_2) dZ_1 = \int_0^1 (F_1^t)^{-1}(u_1) \cdot c^t(u_1 | u_2) du_1. \quad (7)$$

30 where  $c^t$  is the conditional copula density function. In the case of constructing bivariate copulas, it can be shown that:



$$c^t(u_1|u_2) = c^t(u_1, u_2) = \frac{\partial^2 c^t(u_1, u_2)}{\partial u_1 \partial u_2}. \quad (8)$$

The expectation predictor (EP) is mostly used for copulas to predict the value at an unvisited location in space (Bárdossy and Li 2008) or to predict the value at an unvisited location in space and time (Gräler and Pebesma 2011) using a large number of observations. In copula-based bias correction methods, however, spatial variability around unvisited locations faces the smoothing effect of EP. Another drawback concerns the marginal quantile  $\hat{u}_1$ . The conditional expectation is either an increasing or a decreasing function of the conditioning variable if the dependence is positive or negative, respectively. Therefore, after applying EP, the empirical marginal quantile  $\hat{u}_1$  equals  $u_2$  or  $1 - u_2$ .

### 2.3.3 Marginal transformation based on a single quantile

The conditional quantile  $p_{u_1}$  specifies that the conditioned variable  $Z_1$  takes a value for a given conditioning variable  $Z_2$ . To apply the marginal transformation based on a single quantile method, first, the same quantile  $p_{u_1}$  for all locations is used to derive the marginal quantile  $\hat{u}_1$ , by applying the inverse transformation of the copula  $(C^t)^{-1}$ :

$$\hat{u}_1 = (C^t)^{-1}(p_{u_1}|u_2). \quad (9)$$

Then the realization of the random variable  $\hat{Z}_1$  is obtained by applying the inverse transformation of its marginal distribution  $(F_1^t)^{-1}$  (Nelsen 2006):

$$\hat{z}_1 = (F_1^t)^{-1}(\hat{u}_1). \quad (10)$$

As the full conditional distribution of variable of interest is derived, any quantiles  $p_{u_1}$  can be used for instance, the median value of  $\hat{Z}_1$  can be obtained when the quantile  $p_{u_1}$  is 0.5 for all locations. In this method, the question can be posed which quantile  $p_{u_1}$  best suits for the corrected variable at unvisited locations.

### 2.3.4 Simulation of conditional quantile

In simulation of conditional quantiles, realizations of the random variable  $\hat{Z}_1$  are obtained by generating independent variates  $u_2$  and  $p_{u_1}$  uniform on  $[0,1]^2$  (Salvadori et al. 2007; Nelsen 2006). These variates are used in Eq. (9) to obtain samples  $\hat{u}_1$ . These samples are transformed to obtain realizations of the random variable  $\hat{Z}_1$  by applying the inverse transformation of the marginal distribution in Eq. (10). Here, to obtain a single value for air temperature, a choice for either the mean, or the median or the mode of a simulation provides a single value  $\hat{z}_1$ . In the literature, the mean value of the simulations is considered as a single realization (Laux et al. 2011; Vogl et al. 2012). The number of samples in the simulations, however, influences the simulation of conditional quantiles. The mean and the median of the simulations are equal to the mean and the median as derived from the conditional copulas using methods 2.3.2 and 2.3.3 when choosing large number of the samples in the simulation (Mao et al. 2015).



### 2.3.5 Bivariate copula quantile mapping

This section introduces new bias correction methods including a covariate to consider the spatial structure of the air temperature at unvisited locations. The bivariate copula quantile mapping (BCQM) is a two dimensional quantile mapping method and relies on two bivariate copulas incorporating the dependence of the covariate and variables of interest (Verhoest et al. 2015).

5 This method can be extended to multi-dimensional quantile mapping using more than one covariate for the air temperature.

#### 2.3.5.1 BCQM-type I

The variables  $R$  and  $u_R$  are defined as:

$$R = \sqrt{(x^s)^2 + (y^s)^2 + (e^s)^2}. \quad (11)$$

$$u_R = \frac{\text{rank}(R)}{k+1}. \quad (12)$$

10 where  $x^s$  and  $y^s$  are the coordinates (in meters) in the universal transverse Mercator (UTM) coordinate system and  $e^s$  is the elevation (in meter) of the unvisited locations. The variable  $R$  is treated as a random variable due to uncertainty in positioning and elevation. It indicates effects of land cover and elevation on the air temperature over the study area. The idea of this mapping is to use  $R$  and the air temperature to estimate copulas. Then, the conditional quantile  $P(Z_2 \leq z_2 | R = r)$  at an unvisited location is used to estimate the conditional quantile  $P(Z_1 \leq z_1 | R = r)$  at the same location. For this quantile mapping, two conditional copulas  $C_{u_R}^t(u_1)$  and  $C_{u_R}^t(u_2)$  are constructed as:

$$P(Z_1 \leq z_1 | R = r) = C_{u_R}^t(u_1) = C^t(u_1 | u_R) = \frac{\partial C^t(u_R, u_1)}{\partial u_R} = p_{u_1}, \quad C: [0,1]^2 \rightarrow [0,1]. \quad (13)$$

$$P(Z_2 \leq z_2 | R = r) = C_{u_R}^t(u_2) = C^t(u_2 | u_R) = \frac{\partial C^t(u_R, u_2)}{\partial u_R} = p_{u_2}, \quad C: [0,1]^2 \rightarrow [0,1]. \quad (14)$$

where  $u_1$  and  $u_2$  are calculated following Eq. (5). Substituting the quantiles  $p_{u_2}$  for  $p_{u_1}$  in Eq. (13) yields the realization of the random variable  $\hat{Z}_1$  as it is explained in Eq. (9) and (10).

#### 20 2.3.5.2 BCQM-type II

The idea of the BCQM-type II method is to use nearest observed neighbour to an unvisited location to estimate copulas. Then, the conditional quantile  $P(Z_2 \leq z_2^s | Z_2 = z_2^{\text{neigh}})$  at an unvisited location is used to estimate the conditional quantile  $P(Z_1 \leq z_1^s | Z_1 = z_1^{\text{neigh}})$  at the same location. For this quantile mapping, two bivariate conditional copulas  $C_{u_1^{\text{neigh}}}^t(u_1^s)$  and  $C_{u_2^{\text{neigh}}}^t(u_2^s)$  are constructed as:

$$25 \quad P(Z_1 \leq z_1^s | Z_1 = z_1^{\text{neigh}}) = C_{u_1^{\text{neigh}}}^t(u_1^s) = C^t(u_1^s | u_1^{\text{neigh}}) = \frac{\partial C^t(u_1^{\text{neigh}}, u_1^s)}{\partial u_1^{\text{neigh}}} = p_{u_1}, \quad C: [0,1]^2 \rightarrow [0,1]. \quad (15)$$

$$P(Z_2 \leq z_2^s | Z_2 = z_2^{\text{neigh}}) = C_{u_2^{\text{neigh}}}^t(u_2^s) = C^t(u_2^s | u_2^{\text{neigh}}) = \frac{\partial C^t(u_2^{\text{neigh}}, u_2^s)}{\partial u_2^{\text{neigh}}} = p_{u_2}, \quad C: [0,1]^2 \rightarrow [0,1]. \quad (16)$$



where  $u_1$  and  $u_2$  are calculated following Eq. (5). The copula  $C_{u_i}^t(u_i^s)$  is the distribution of variable of interest at unvisited location, conditioned on its nearest neighbour. Substituting the quantiles  $p_{u_2}$  for  $p_{u_1}$  in Eq.(15) yields the realization of the random variable  $\hat{Z}_1$  as it is explained in Eq. (9) and (10).

### 2.3.6 Quantile search

- 5 The quantile search (QS) method allows the combination of different criteria in estimating the marginal quantiles  $u_1$  at unvisited locations. A realization of the random variable  $\hat{Z}_1^{t,s}$  is obtained using a marginal transformation in Eq. (10) based on the estimated quantiles at unvisited locations in Eq. (9). As the marginal quantile  $u_1$  lies in the range  $[0, 1]$ , it can be estimated using a search algorithm by means of maximizing a fitness function  $f$  as:

$$\hat{p}_{u_1} = \hat{C}_*(\hat{u}_1); \quad *: \{u_2, u_R, u_1^{neigh}\}. \quad (17)$$

$$10 \quad RE_* = \frac{|\hat{p}_{u_1} - p_{u_1}|}{p_{u_1}}; \quad MRE_* = \frac{1}{n} \sum_{s=1}^n (RE_*^s). \quad (18)$$

$$f(\hat{u}_1) = -\sum w_* \times MRE_*. \quad (19)$$

- Here  $\hat{p}_{u_1}$  and  $\hat{u}_1$  are conditional and marginal quantiles estimated by the quantile search,  $w_*$  is arbitrary weight set equal to 0.33 in this study,  $MRE_*$  is the mean relative error,  $n$  is number of weather stations, and  $RE_{u_2}$  is the relative error between two quantiles of  $C_{u_2}^t(u_1)$  and  $\hat{C}_{u_2}^t(\hat{u}_1)$  as explained in the Sect. 2.2.  $RE_{u_R}$  is the relative error between two quantiles of  $C_{u_e}^t(u_1)$  and  $\hat{C}_{u_e}^t(\hat{u}_1)$  as explained in the Sect. 2.3.5.1.  $RE_{u_1^{neigh}}$  is the relative error between two quantiles of  $C_{u_1^{neigh}}^t(u_1)$  and  $\hat{C}_{u_1^{neigh}}^t(\hat{u}_1)$  as explained in the Sect. 2.3.5.2. The  $MRE$  ensures that the prediction's errors are minimized at the weather stations. The  $RE_*$  allows us to ensure that dependence structure of the observed and forecasted variables as well as the observed variable and covariates are considered in the finding the marginal quantile. Values of the fitness function  $f(\hat{u}_1)$  are calculated using initial random values for  $\hat{u}_1$  and the search algorithm improve the quantile  $\hat{u}_1$  in an iterative process. Therefore, the fitness values should well represent the estimation errors and the dependence structures at unvisited locations. Here, we applied a genetic algorithm for doing the search.

### 2.4 Evaluation of the copula-based bias correction methods

- The newly developed methods are applied to each time step of the air temperature time series. These time steps represent different bias and dependencies structures between the observed and forecasted variables. The observations from weather stations are used for cross-validation to quantify the robustness of the each method. To this end, one observation  $z_1^{s,t}$  is removed from the dataset and the bias-corrected value  $\hat{z}_1^{s,t}$  is calculated for this point using the reminder of the stations. This method is repeated for all stations. For each observation assigned to the one location  $s$  and time  $t$ , that is not included in the bias correction process, the absolute error (AE) is determined, using:

$$AE^{s,t} = |\hat{z}_1^{s,t} - z_1^{s,t}|. \quad (20)$$





The spatial mean absolute error (SMAE) is calculated at each weather station as:

$$SMAE^s = \frac{1}{T} \sum_{t=1}^T (AE^{s,t}). \quad (21)$$

To compare the five bias correction methods, an error score (ES) is calculated based on the SMAE for each method at each weather station (Durai and Bhadrwaj 2014). A minimum value of the error score indicates for the minimum SMAE. The error measures do not provide any spatial information of the bias-corrected variable. The idea behind the SMAE was to provide criteria when one can compare different methods. A low number of observations can hinder a deeper analysis. The overall prediction quality depends on a good model of the copula, a good fit of the marginal distributions as well as the number of the observations.

In addition, the correlation coefficient (CC) between observed and bias-corrected values is calculated at each weather station as:

$$CC^s = \frac{cov\{Z_1^s, \hat{Z}_1^s\}}{\sigma_{Z_1^s} \sigma_{\hat{Z}_1^s}}; \quad Z_1^s = \{z_1^{s,1}, z_1^{s,2}, \dots, z_1^{s,T}\}, \quad \hat{Z}_1^s = \{\hat{z}_1^{s,1}, \hat{z}_1^{s,2}, \dots, \hat{z}_1^{s,T}\}. \quad (22)$$

Where  $Z_1^s$  is the observation values and  $\hat{Z}_1^s$  is the biased-corrected values obtained by cross-validation. To compare the five bias correction methods, an correlation score (CS) is calculated based on the CC for each method at each weather station. A minimum value of the correlation score indicates for the minimum CC.

For investigating the performance of each method to reproduce the high moments of the marginal distribution, the relative error  $RE^{mi}$  is calculated as:

$$RE^{mi,t} = \frac{|m_i^t - \hat{m}_i^t|}{|m_i^t|}. \quad (23)$$

where  $m_i^t$  and  $\hat{m}_i^t$  are the  $i^{th}$  order moment of the marginal distribution calculated using observed values  $z_1$  and bias-corrected values  $\hat{z}_1$  at time  $t$ . The bias-corrected values  $\hat{z}_1$  are predicted where correction functions are estimated using the observed values and applied to the same locations (Lafon et al. 2013).

The moment mean relative error (MMRE) is calculated at each weather station as:

$$MMRE^{mi} = \frac{1}{T} \sum_{t=1}^T (RE^{mi,t}). \quad (24)$$

To compare the five bias correction methods, an error score (ES) is calculated based on the MMRE for each method and for each moment. A minimum value of the error score indicates for the minimum MMRE.

The study was performed in the statistical computing environment and language R using the packages gstat (Pebesma 2004), copula (Kojadinovic and Yan 2010), spcopula (Gräler 2011), VineCopula (Brechmann and Schepsmeier 2013), GA (Scrucca 2012) and the basic packages.

### 3 Case study

The study area is located between 36.30 and 35.99 latitudes ( $N$ ) and 49.64 and 50.59 longitudes ( $E$ ), with a total area of 3307 km<sup>2</sup> in the Qazvin plain, Iran (Figure 1). This area includes an irrigation network, agricultural fields, dominated by wheat,





- barely, maize, sugar beet, summer crops and orchards, urban areas, bare soil and natural vegetation. Part of this area has been the pilot for a project aiming at development of a planning and monitoring system to support irrigation management of the Qazvin irrigation network (Sharifi 2013). One of the objectives of this project is to produce air temperature map from point measurements and apply it to crop growth simulations.
- 5 Five weather stations (Table 2) were selected because they had a long range of air temperature measurements available and were well spread over the study area. Minimum and maximum distances between stations are 13 and 78 km, respectively (Figure 1). For all weather stations, the daily minimum and maximum air temperatures are available for the periods 1– 31 March and 1–30 June 2014, except for the second station on 20 March and 23 June and for the first station on 30 June. Daily air temperature is determined by averaging the minimum and maximum temperatures at each weather stations for each day.
  - 10 We used the operational forecast weather data provided by the European Centre for Medium-Range Weather Forecasts (ECMWF). All ECMWF data are available at 3-hourly and 6-hourly intervals from the ERA-Interim data assimilation system and can be retrieved for a  $0.125^\circ$  lat/lon grid points, corresponding to approximately 13.5 km in the meridional direction (Persson 2013). A sample subset of  $3 \times 8$  grid points is selected for the periods 1– 31 March and 1– 30 June 2014 which covers the irrigation network (Figure 1).
  - 15 Due to the coarse spatial resolution of ECMWF data, there is an apparent mismatch between measurements obtained from weather stations and weather forecast data. To correct for bias in weather forecast data, either an observed value or the average of several observed values corresponds to a single grid point if distance between the station and the grid point is negligible. In the study area, however, many grid points do not contain an observation due to the relatively low number of weather stations. In order to obtain unbiased values, a bias correction method should be applied for these grid points before using the weather
  - 20 forecast data.

## 4 Results

- This section presents the results, where the observed values are the daily air temperatures at five weather stations, forecasted values are the daily air temperatures obtained from ECMWF, and the bias-corrected values are the results of the bias correction methods (MQM, EP, BCQM-type I, BCQM-type II and QS) for twenty-four grid points during the periods 1– 31 March and
- 25 1– 30 June 2014.

### 4.1 Outlier and bias

- The graphical comparison of the observed and the forecasted time series of temperature as shown in Figure 2 identifies both bias and outliers. Abrupt changes in the trend correspond to the outliers (Aggarwal 2013). As can be seen, when there is a drop of the observed air temperature, the forecast system produces outliers. Figure 3 shows the scatterplot between the observed
- 30 and the forecasted values at each weather station. For all stations, outliers occurred on days 8, 19, 22 and 31 in March. The



forecasted values are negative on days 22 and 31 in March. Since bias correction was applied separately for each day, there was no need to remove the outliers.

In addition, the graphical comparison in Figure 2 reveals that the daily air temperature is underestimated by ECMWF. The extrapolation of climate information from uncertain measurements and time-varying bias in the ECMWF models and observations are associated with uncertainties in the forecasted data (Dee et al. 2011). The average of bias for all days is 3.4°C if the outliers (on the days 8, 19, 22 and 31) are ignored and 4.1°C in March and June, respectively. Figure 4 shows the mean, sample standard deviation, skewness and kurtosis for both observed and forecasted values at each day. This figure shows, in time, clearly visible bias in all moments of the marginal distribution. Classical bias correction methods are inadequate to improve all order moments of the marginal distribution (Lafon et al. 2013). In Sect. 4.3, we investigate how well the moments can be reproduced by the described methods.

## 4.2 Marginal distributions and copulas

In order to not affect the copula by the estimation of the marginal distribution functions, the empirical marginal values  $u_1$  and  $u_2$  were calculated using the available data for both observed and forecasted air temperature for each day as mentioned in Sect. 2.2. The empirical quantiles, however, are typically limited to the domain defined by the extreme values in the observations. A third degree polynomial was fitted to the empirical marginal quantiles  $u_1$  to extend the marginal quantiles towards the unvisited locations as well. The empirical marginal quantiles and the fitted polynomials are presented in Figure 5 for first day of March and June.

The bivariate conditional copulas were fitted to the empirical marginal quantiles for each day. Following Sect. 2.2, five families were estimated at each day and the most suitable family was selected according to AIC. Table 3 shows the best families and Kendall's  $\tau$  at each day in March and June. As can be seen, suitable families of the dependence between the observed and forecasted variables were non-Gaussian at most of days in March and Gaussian at most of days in June and these families covered the range from negative to positive dependences. The selection of families, however, depends upon the number of observations and further research is needed to develop strategies to select them. In addition, as all five families were symmetric, alternative families can be investigated to better describe the dependencies. It must be mentioned that although many different families exist allowing for different dependence structures, the computational limitations may be introduced by the calculating the inverse of the conditional copula distribution.

## 4.3 Cross-validation results and the bias-corrected values $\hat{z}_1$

Applying the described methods to the same data allowed us to compare the different underlying definitions. Table 4 shows the cross-validation results in terms of the spatial mean absolute error (SMAE) between the observations and the bias-corrected values at each weather stations for five bias correction methods and their scores. A comparison between the newly developed methods BCQM-type I, BCQM-type II, QS, available copula-based method EP and classical bias correction method MQM



based upon the error scores (ES) has shown that QS performed best, followed by EP, MQM and BCQM-type I, BCQM-type II, in March and June.

Table 5 shows the cross-validation results in terms of the correlation coefficient (CC) between the observations and the bias-corrected values at each weather stations for five bias correction methods and their scores. A comparison between the newly developed methods BCQM-type I, BCQM-type II, QS, available copula-based method EP and classical bias correction method MQM based upon the correlation score (CS) has shown that QS performed best, followed by BCQM-type II, MQM, EP and BCQM-type I, in March and June.

The first station has the largest temperature values in both March and June, the second and the fifth stations have the smallest temperature values in March, the third and the fifth stations have the smallest temperature values in June, among the five stations, at most of days. Since for all methods, the empirical marginal distributions were the same, the copulas were unable to capture the extreme values. In addition, the SMAE represents the uncertainties associated to horizontal distances, height differences, differences in land cover and vegetation coverage between the stations and the grid points.

Table 6 shows the moment mean relative error (MMRE) between the observations and the bias-corrected values at each weather stations for five bias correction methods and their scores. A comparison between the newly developed methods BCQM-type I, BCQM-type II, QS, available copula-based method EP and classical bias correction method MQM based upon the error score (ES) has shown that QS performed best, followed by EP, BCQM-type II, MQM, and BCQM-type I, in March and June.

The spatial variabilities of the bias-corrected variable at some days for all locations is shown in Figure 6 and Figure 7 for March and June, respectively. It can be seen that the spatial variabilities obtained by newly developed methods were much higher than by MQM and EP. MQM, BCQM-type I and BCQM-type II were unable to correct for bias at some locations. The smoothing effect of EP can be seen in days 6 and 13 in Figure 6, as well. The spatial variabilities of bias-corrected values obtained by MQM and EP follow the spatial variabilities of the forecasted values. QS performed better at the weather stations due to the fitness function in Sect. 2.3.7. How to analyse the spatial variability of the bias-corrected air temperature at unvisited locations is still a challenging question due to low number of observations.

## 5 Discussion

The dependence structure between the daily air temperature observed by the weather stations and forecasted by ECMWF was studied for bias correction. We utilized the concept of bivariate conditional copula to develop three new methods in the bias correction methods, as bivariate copulas are well understood and easy to estimate. We picked up the idea of the quantile mapping and adapted it to the bivariate conditional copula to develop the new methods BCQM-type I and BCQM-type II that allow estimating different conditional quantiles at different unvisited locations. The flexibility in the determining of the conditional quantiles makes the newly developed methods appealing for spatial variabilities at unvisited locations when low number of observations are available. The estimation of marginal distributions and copulas, however, are affected by the low



number of observations. In addition, the new quantile search QS was proposed to find the marginal quantiles that might benefit from a fitness function that does not only take into account the prediction errors, but also the spatial variabilities at the unvisited locations. Furthermore, our proposed methods utilized the flexibility of selecting different families and allowed for temporal variability of dependencies.

- 5 We treated the available observations from five weather stations as a reference during the identification of bias and during the validation of the results. The horizontal distances, height differences and difference in land cover between the location of a station and the ECMWF grid point is associated with uncertainties. In addition, in the copula-based methods, where we used the AIC to select the suitable family for constructing the dependence between the forecasted and the observed variables, additional uncertainties present because the suitability of family depends on the availability of data and the probabilistic nature
- 10 of the bias. Furthermore, based on the cross-validation results, the average of the mean absolute errors in all stations and all days appeared to be slightly more than 1°C for all proposed methods. As mentioned in Sect. 3, the bias-corrected air temperature can be used for crop growth simulation as well as determination of crop water requirement. The impact of air temperature variability on crop production is dependent on growing-season temperature and the optimum temperature for photosynthesis and biomass accumulation. Asseng et al. 2011 showed that, depending on the time and temperature, the
- 15 variation in the average growing-season temperature could cause a significant reduction in wheat grain production. A practical advantage of the proposed methods is that they are not restricted to remove autocorrelation and heteroscedasticity in time series (Laux et al. 2011) and the time series of the air temperature at each station were successfully reproduced by applying the bias correction separately at each day. Another aspect is the ability of the new methods to reproduce the moments of the marginal distribution of the observed variable. Correction of the higher moments of the distribution is much more
- 20 sensitive to the choice of the bias correction method, which needs to be investigated more in further studies. In addition, in the proposed methods, the empirical marginal distribution described the statistical properties of daily air temperature without the knowledge of theoretical form of the family's distribution function. Furthermore, fitting a polynomial to the empirical marginal quantiles was beneficial to obtain the bias-corrected values at unvisited locations that were not limited to the domain defined by the extreme values in the observations. With respect to the newly described methods, although we applied the methods for
- 25 correcting the bias, we highlight the potential and the use of the methods for the copula-based downscaling problems, as well. Moreover, the proposed methods have the potential to use the spatio-temporal information of the variable of interest in the bias correction process. The further comparison of the proposed methods and other bias correction methods e.g. triple collocation analysis (Stoffelen 1998) might help to assess the performance of the newly developed methods.
- 30 Lack of spatial variability in the available copula-based bias correction methods motivated the research to develop new methods with the aim of estimating different conditional quantiles at different locations. The spatial variability of the air temperature, however, needs additional analysis, as the number of observations is small. Based on the available literature, estimating the confidence intervals is a common task to address the uncertainties in the copula-based methods. The applicability of confidence intervals, however, always depends on the availability of data and the nature of the real world problem. In addition, for the BCQM-type I and BCQM-type II methods it is assumed that the associations between the pair of



the bias-corrected variable and a covariate should obey the associations between the pair of the biased variable and that covariate. For QS method it is assumed that the fitness function fitted to the observations is an acceptable representation of fitness function at unvisited locations. In the case the underlying assumptions of these methods are hard to be fulfilled, alternatives are needed.

## 5 6 Conclusions

In this paper, we developed three copula-based bias correction methods with the aim of predicting different conditional quantiles at unvisited locations and compared them to available methods. They were applied to correct bias in the daily air temperature forecasts of ECMWF. To evaluate their performance, cross-validation was carried out with the observations from five weather stations.

10 From this study, we conclude the following:

- The new methods are beneficial for the local refinement of weather data if a low number of observations is available and one is interested in predicting the spatial variabilities of the weather parameter.
- The new methods are advantageous if the bias-corrected variable has to be predicted separately at each time step of the time series.
- 15 • Further research should focus on investigating the optimal number of observations for bias correction and on developing validation criteria. In both issues, the spatial variability and the error of the predictions in case of a low number of observations should be included.

## Competing interests

The authors declare that they have no conflict of interest.

## 20 Acknowledgements

The authors acknowledge the European Centre for Medium-Range Weather Forecasts (ECMWF) for providing weather forecast data and the SAJ Consulting firm in Iran for providing weather stations data.

## References

- Aggarwal, C. C.: Outlier Analysis, Springer-Verlag New York, 456 pp., 2013.
- 25 Akaike, H.: A New Look at the Statistical Model Identification., IEEE Trans. Autom. Control, 19, 716-723, doi:10.1109/TAC.1974.1100705, 1974.



- Asseng, S., Foster, I., and Turner, N. C.: The impact of temperature variability on wheat yields., *Global Change Biology* 17, 997–1012, doi:10.1111/j.1365-2486.2010.02262.x, 2011.
- Bárdossy, A., and Li, J.: Geostatistical interpolation using copulas, *Water Resour. Res.*, 44, 15, doi:10.1029/2007WR006115, 2008.
- 5 Brechmann, E. C., and Schepsmeier, U.: Modeling Dependence with C- and D-Vine Copulas: The R Package CDVine, *Journal of Statistical Software*, 52, 1-27, doi:10.18637/jss.v052.i03, 2013.
- Cressie, N.: *Spatial prediction and Kriging in: Statistics for Spatial Data*, John Wiley & Sons, Canada, 105-110, 1993.
- Dee, D. P., Uppala, S. M., Simmons, A. J., Berrisford, P., Poli, P., Kobayashi, S., Andrae, U., Balmaseda, M. A., Balsamo, G., Bauer, P., Bechtold, P., Beljaars, A. C. M., van de Berg, L., Bidlot, J., Bormann, N., Delsol, C., Dragani, R., Fuentes, M.,
- 10 Geer, A. J., Haimberger, L., Healy, S. B., Hersbach, H., Holm, E. V., Isaksen, L., Kallberg, P., Kohler, M., Matricardi, M., McNally, A. P., Monge-Sanz, B. M., Morcrette, J. J., Park, B. K., Peubey, C., Rosnay, P. d., Tavolato, C., Thepaut, J. N., and Vitart, F.: The ERA-Interim reanalysis: configuration and performance of the data assimilation system., *Q. J. R. Meteorol. Soc.*, 137, 553-597, doi:10.1002/qj.828, 2011.
- Demarta, S., and McNeil, A. J.: The t copula and related copulas., *International Statistical Review/Revue Internationale de*
- 15 *Statistique*, 73, 111-129, 2005.
- Durai, V. R., and Bhradwaj, R.: Evaluation of statistical bias correction methods for numerical weather prediction model forecasts of maximum and minimum temperatures., *Nat. Hazards*, 73, 1229-1254, doi:10.1007/s11069-014-1136-1, 2014.
- Genest, C., and Favre, A.-C.: Everything You Always Wanted to Know about Copula Modeling but Were Afraid to Ask., *Journal of Hydrologic Engineering* 12, 347-368, 2007.
- 20 Statistics <http://r-forge.r-project.org/projects/spcopula>, 2011.
- Gräler, B., and Pebesma, E.: The pair-copula construction for spatial data: a new approach to model spatial dependency., *Procedia Environ. Sci.*, 7, 206-211, 2011.
- Ines, A. V. M., and Hansen, J. W.: Bias correction of daily GCM rainfall for crop simulation studies., *Agric. For. Meteorol.*, 138, 44-53, doi:10.1016/j.agrformet.2006.03.009, 2006.
- 25 Joe, H.: Parametric families of multivariate distributions with given margins. , *Journal of Multivariate Analysis*, 46, 262-282, 1993.
- Kojadinovic, I., and Yan, J.: Modeling Multivariate Distributions with Continuous Margins Using the copula R Package., *Journal of Statistical Software*, 34, 1–20, 2010.
- Kum, D., Lim, K. J., Jang, C. H., Ryu, J., Yang, J. E., Kim, S. J., Kong, D. S., and Jung, Y.: Projecting Future Climate Change
- 30 *Scenarios Using Three Bias-Correction Methods.*, Hindawi Publishing Corporation *Advances in Meteorology*, 2014, 1-13, doi:10.1155/2014/704151, 2014.
- Lafon, T., Dadson, S., Buys, G., and Prudhomme, C.: Bias correction of daily precipitation simulated by a regional climate model: a comparison of methods, *International Journal of Climatology*, 33, 1367-1381, doi:10.1002/joc.3518, 2013.



- Laux, P., Vogl, S., Qiu, W., Knoche, H. R., and Kunstmann, H.: Copula-based statistical refinement of precipitation in RCM simulations over complex terrain, *Hydrol. Earth Syst. Sci.*, 15, 2401-2419, doi:10.5194/hess-15-2401-2011, 2011.
- Lenderink, G., Buishand, A., and van Deursen, W.: Estimates of future discharges of the river Rhine using two scenario methodologies: direct versus delta approach *Hydrol. Earth Syst. Sci.*, 11, 1145-1159, doi:10.5194/hess-11-1145-2007, 2007.
- 5 Manner, H.: Estimation and Model Selection of Copulas with an Application to Exchange Rates, Maastricht research school of Economics of TEchnology and ORganizations, Universiteit Maastricht, 1-37, 2007.
- Mao, G., Vogl, S., Laux, P., Wagner, S., and Kunstmann, H.: Stochastic bias correction of dynamically downscaled precipitation fields for Germany through Copula-based integration of gridded observation data, *Hydrol. Earth Syst. Sci.*, 19, 1787-1806, doi:10.5194/hess-19-1787-2015, 2015.
- 10 Nelsen, R. B.: An Introduction to Copulas, Springer, United States of America, 276 pp., 2006.
- Pebesma, E. J.: Multivariable geostatistics in S: the gstat package, *Comput. Geosci.*, 30, 683-691, doi:10.1016/j.cageo.2004.03.012, 2004.
- Persson, A.: User guide to ECMWF forecast products, Livelink 4320059, 2013.
- Salvadori, G., De Michele, C., Kotegoda, N. T., and Rosso, R.: *Extremes In Nature: An Approach Using Copulas*, edited by: V.P. Singh, T. A. M. U., College Station, U.S.A., Springer, P.O. Box 17, 3300 AA Dordrecht, The Netherlands, 2007.
- 15 Scrucca, L.: GA: A Package for Genetic Algorithms in R. *Journal of Statistical Software*, 53, 1-37, 2012.
- Sharifi, M.: Development of planning and monitoring system supporting irrigation management in the Ghazvin irrigation network, SAJ Co. , Tehran, Iran, 2013.
- Sklar, A.: Random variables, joint distribution functions, and copulas, *Kybernetika*, 9, 449-460, 1973.
- 20 Stoffelen, A.: Toward the true near-surface wind speed: Error modeling and calibration using triple collocation, *J. Geophys. Res.: Atmos.*, 103, 7755-7766, doi:10.1029/97JC03180, 1998.
- Teutschbein, C., and Seibert, J.: Bias correction of regional climate model simulations for hydrological climate-change impact studies: Review and evaluation of different methods, *Journal of Hydrology*, 456-457, 12-29, 2012.
- Verhoest, N. E. C., Berg, M. J. v. d., Martens, B., Lievens, H., Wood, E. F., Pan, M., Kerr, Y. H., Al Bitar, A., Tomer, S. K.,
- 25 Drusch, M., Vernieuwe, H., De Baets, B., Walker, J. P., Dumedah, G., and Pauwels, V. R. N.: Copula-Based Downscaling of Coarse-Scale Soil Moisture Observations With Implicit Bias Correction, *IEEE Trans. Geosci. Remote Sens.*, 53, 3507-3521, doi:10.1109/TGRS.2014.2378913, 2015.
- Vogl, S., Laux, P., Qiu, W., Mao, G., and Kunstmann, H.: Copula-based assimilation of radar and gauge information to derive bias-corrected precipitation fields, *Hydrol. Earth Syst. Sci.*, 16, 2311-2328, doi:10.5194/hess-16-2311-2012, 2012.





**Table 1:** Five families are selected to describe the dependence structure between the conditioned and the conditioning variables in this study. A bivariate copula is fitted on the marginal values and the most suitable family is selected according to the Akaike Information Criteria for each day.

Index	Name	$C\theta(u,v)$	Property index
1	Gaussian	$\Phi_R(\Phi^{-1}(u), \Phi^{-1}(v)); R = \begin{bmatrix} 1 & \theta \\ \theta & 1 \end{bmatrix}$	1, 2, 6
2	Student's $t$	$t_{R,\vartheta}(t_{\vartheta}^{-1}(u), t_{\vartheta}^{-1}(v)); R = \begin{bmatrix} 1 & \theta \\ \theta & 1 \end{bmatrix}; \vartheta = \text{degree of freedom}$	1, 2, 6
3	Clayton	$[\max\{(u^{\theta} + v^{\theta} - 1), 0\}]^{\frac{-1}{\theta}}$	1, 2, 4, 5, 6
4	Gumbel	$\exp(-[(-\ln u)^{\theta} + (-\ln v)^{\theta}]^{\frac{1}{\theta}})$	1, 2, 3, 6
5	Frank	$\frac{-1}{\theta} \ln(1 + \frac{(e^{-\theta u} - 1)(e^{-\theta v} - 1)}{e^{-\theta} - 1})$	1, 2, 6
1	Property	Permutation symmetry	
2		Symmetry about medians	
3		Extreme value Copula	
4		Lower tail dependence	
5		Upper tail dependence	
6		Extendibility to Multivariate Copula	

**Table 2:** Five weather stations are selected due to the air temperature measurements available over the entire study area. For all weather stations, minimum and maximum air temperatures are available for the periods 1– 31 March and 1-30 June 2014, except for the second station on 20 March and 23 June and for the first station on 30 June.

Station ID	Station name	Latitude	Longitude	Elevation(m)	Type
1	Abeyk	36.05	50.52	1291	Climatology
2	Magsal	36.13	50.12	1260	Climatology
3	Nirougah	36.18	50.25	1318	Climatology
4	Qazvin	36.25	50.05	1278	Synoptic
5	Takestan	36.05	49.65	1283	Synoptic



**Table 3: Best fitting family and Kendall's  $\tau$  at each day for bivariate conditional copulas  $C_{u_2}^t(u_1)$ . The non-Gaussian bivariate copulas dominate the non-spatial dependence structure of the observed and forecasted variables at most of the days in March.**

Day	March		June	
	Best	Kendall's $\tau$	Best	Kendall's $\tau$
1	Gaussian	-0.39	Gaussian	0.52
2	Clayton	0.56	Gumbel	0.67
3	Gaussian	-0.40	Gaussian	0.74
4	Frank	0.51	Gaussian	0.24
5	Frank	0.63	Gumbel	0.38
6	Gaussian	0.16	Clayton	0.63
7	Gumbel	0.60	Gumbel	0.53
8	Clayton	0.40	Gaussian	0.13
9	Gaussian	-0.46	Gumbel	0.40
10	Gaussian	0.34	Gaussian	-0.45
11	Gumbel	0.46	Gaussian	-0.52
12	Gaussian	0.35	Gaussian	-0.58
13	Gaussian	0.10	Gaussian	-0.29
14	Frank	-0.34	Clayton	0.41
15	Clayton	0.21	Gumbel	0.63
16	Clayton	0.41	Gumbel	0.73
17	Frank	-0.52	Gaussian	-0.61
18	Clayton	0.30	Gaussian	-0.51
19	Gumbel	0.72	Gaussian	-0.47
20	Gumbel	0.45	Gaussian	0.53
21	Gaussian	-0.40	Gaussian	-0.44
22	Gaussian	-0.53	Gumbel	0.52
23	Gumbel	0.54	Gumbel	0.42
24	Gaussian	-0.32	Gumbel	0.59
25	Gaussian	-0.52	Gumbel	0.53
26	Gumbel	0.60	Gaussian	0.45
27	Clayton	0.73	Gumbel	0.66
28	Gaussian	0.61	Gumbel	0.61
29	Gaussian	-0.15	Gaussian	-0.42
30	Gaussian	0.12	Gaussian	-0.68
31	Clayton	0.50		



5 **Table 4: The cross-validation results, which show the robustness of the proposed bias correction methods. The SMAE illustrates the mean absolute errors of all days at each station obtained by the marginal quantile mapping, the expectation predictor, bivariate copula quantile mapping (type I and II), and the quantile search. The last row of the SMAE is the average of SMAE over the study area. To compare the five bias correction methods, an error score (ES) is calculated based on the SMAE for each method at each weather station. A minimum value of the error score indicates for the minimum SMAE. The last row of the ES is the sum of scores for each method and indicates that the quantile search performs better.**

SMAE							ES					
March	Station	MQM	EP	BCQM-I	BCQM-II	QS	Station	MQM	EP	BCQM-I	BCQM-II	QS
	1	1.7	1.5	1.6	1.7	1.5	1	4	2	3	5	1
	2	1.1	1.3	1.2	1.6	1.2	2	1	4	2	5	3
	3	1.0	0.9	1.0	0.9	0.8	3	5	3	4	2	1
	4	1.5	1.2	2.0	1.4	0.6	4	4	2	5	3	1
	5	1.9	1.2	2.5	1.6	1.0	5	4	2	5	3	1
	Average	1.4	1.3	1.6	1.5	1.0	Sum	18	13	19	18	7
June	1	0.9	1.7	1.0	0.9	1.4	1	2	5	3	1	4
	2	1.1	1.1	1.0	1.5	1.1	2	4	3	1	5	2
	3	1.0	1.1	1.0	1.1	0.9	3	3	4	2	5	1
	4	0.7	0.8	0.9	0.8	0.7	4	2	3	5	4	1
	5	1.3	1.2	2.3	1.4	1.0	5	3	2	5	4	1
	Average	1.0	1.2	1.3	1.1	1.0	Sum	14	17	16	19	9



**Table 5:** The correlation coefficient (CC) between observed and bias-corrected values is calculated at each weather station. The bias-corrected values are obtained by the marginal quantile mapping, the expectation predictor, bivariate copula quantile mapping (type I and II), and the quantile search for all days. To compare the five bias correction methods, a correlation score (CS) is calculated based on the CC for each method at each weather station. A minimum value of the error score indicates for the minimum CC. The last row of the ES is the sum of scores for each method and indicates that the quantile search performs better.

5

CC							CS					
	Station	MQM	EP	BCQM -I	BCQM -II	QS	Station	MQM	EP	BCQM- I	BCQM- II	QS
March	1	0.90	0.94	0.92	0.93	0.95	1	1	4	2	3	5
	2	0.92	0.92	0.88	0.94	0.88	2	4	3	1	5	2
	3	0.91	0.90	0.90	0.93	0.93	3	3	1	2	4	5
	4	0.84	0.90	0.82	0.87	0.97	4	2	4	1	3	5
	5	0.66	0.83	0.73	0.76	0.93	5	1	4	2	3	5
							Sum	11	16	8	18	22
June	1	0.88	0.81	0.87	0.88	0.87	1	4	1	2	5	3
	2	0.95	0.92	0.94	0.93	0.92	2	5	1	4	3	2
	3	0.92	0.92	0.91	0.90	0.94	3	4	3	2	1	5
	4	0.96	0.96	0.94	0.95	0.97	4	3	4	1	2	5
	5	0.89	0.91	0.78	0.88	0.94	5	3	4	1	2	5
							Sum	19	13	10	13	20



**Table 6:** For investigating the performance of each method to reproduce the high moments of the marginal distribution, the moment mean relative error (MMRE) is calculated. To compare the five bias correction methods, an error score (ES) is calculated based on the MMRE for each method at each weather station. A minimum value of the error score indicates for the minimum MMRE. The last row of the ES is the sum of scores for each method and indicates that the quantile search performs better.

MMRE							ES					
	Moment	MQM	EP	BCQM -I	BCQM -II	QS	Moment	MQM	EP	BCQM- I	BCQM- II	QS
March	Mean	0.02	0.01	0.03	0.04	0.01	Mean	3	1	4	5	2
	Standard deviation	0.49	0.35	0.61	0.49	0.10	Standard deviation	4	2	5	3	1
	Skewness	1.76	1.61	1.51	1.52	0.62	Skewness	5	4	2	3	1
	Kurtosis	0.39	0.32	0.38	0.34	0.15	Kurtosis	5	2	4	3	1
							Sum	17	9	15	14	5
June	Mean	0.01	0.01	0.01	0.02	0.01	Mean	3	1	4	5	2
	Standard Deviation	0.41	0.48	0.69	0.31	0.14	Standard Deviation	3	4	5	2	1
	Skewness	1.74	1.07	1.73	1.60	0.43	Skewness	5	2	4	3	1
	Kurtosis	0.20	0.21	0.24	0.22	0.08	Kurtosis	2	3	5	4	1
							Sum	13	10	18	14	5

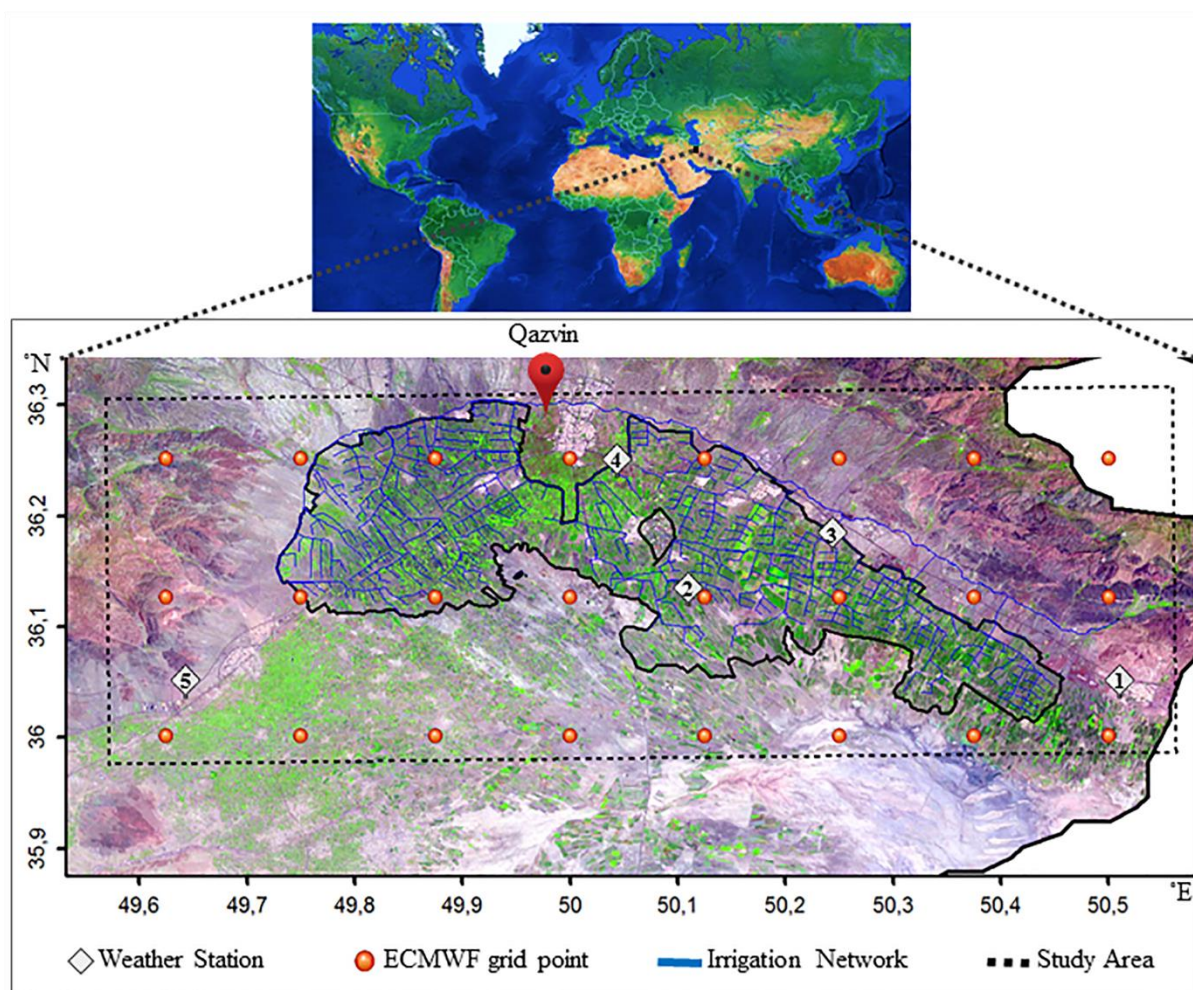
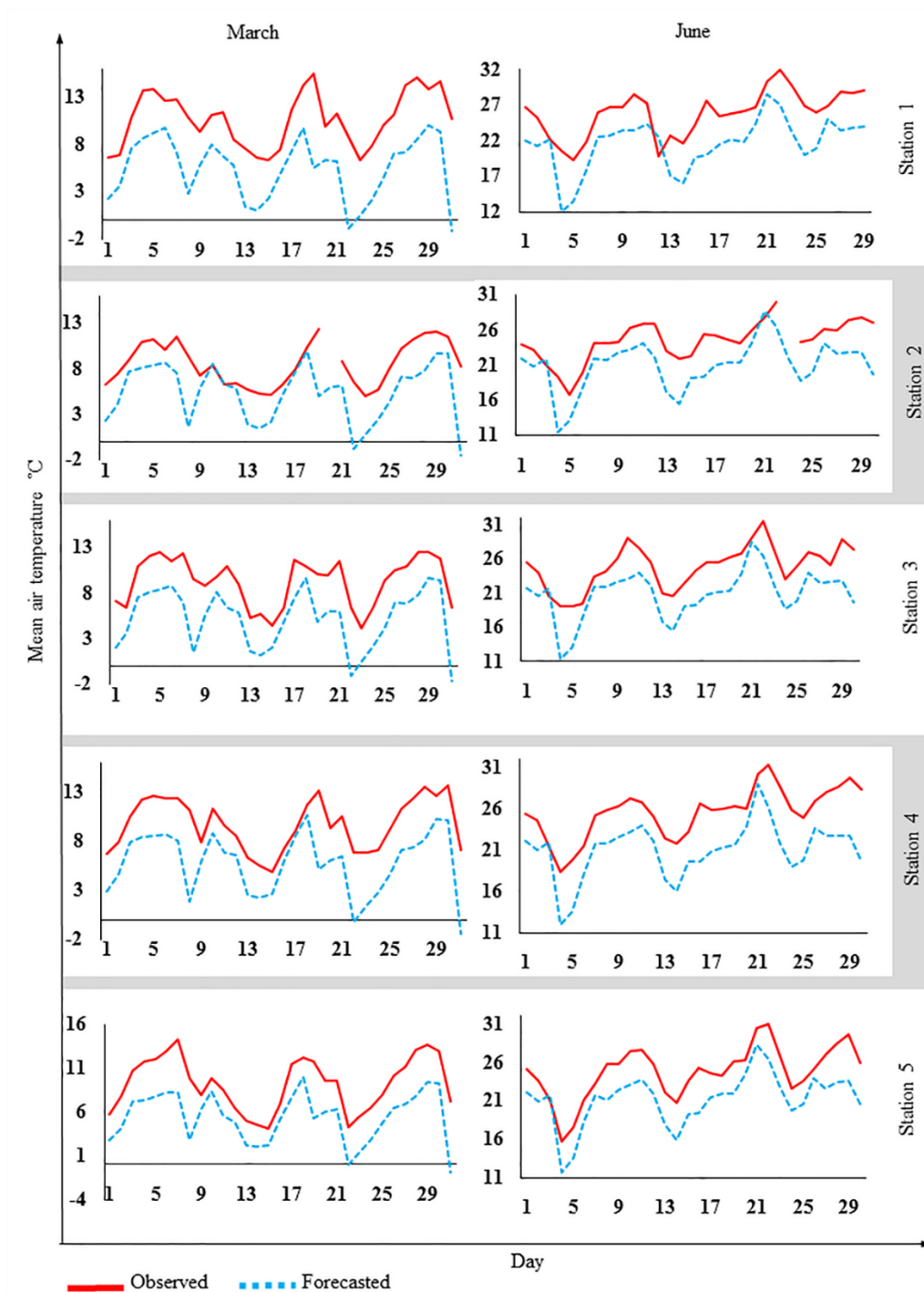
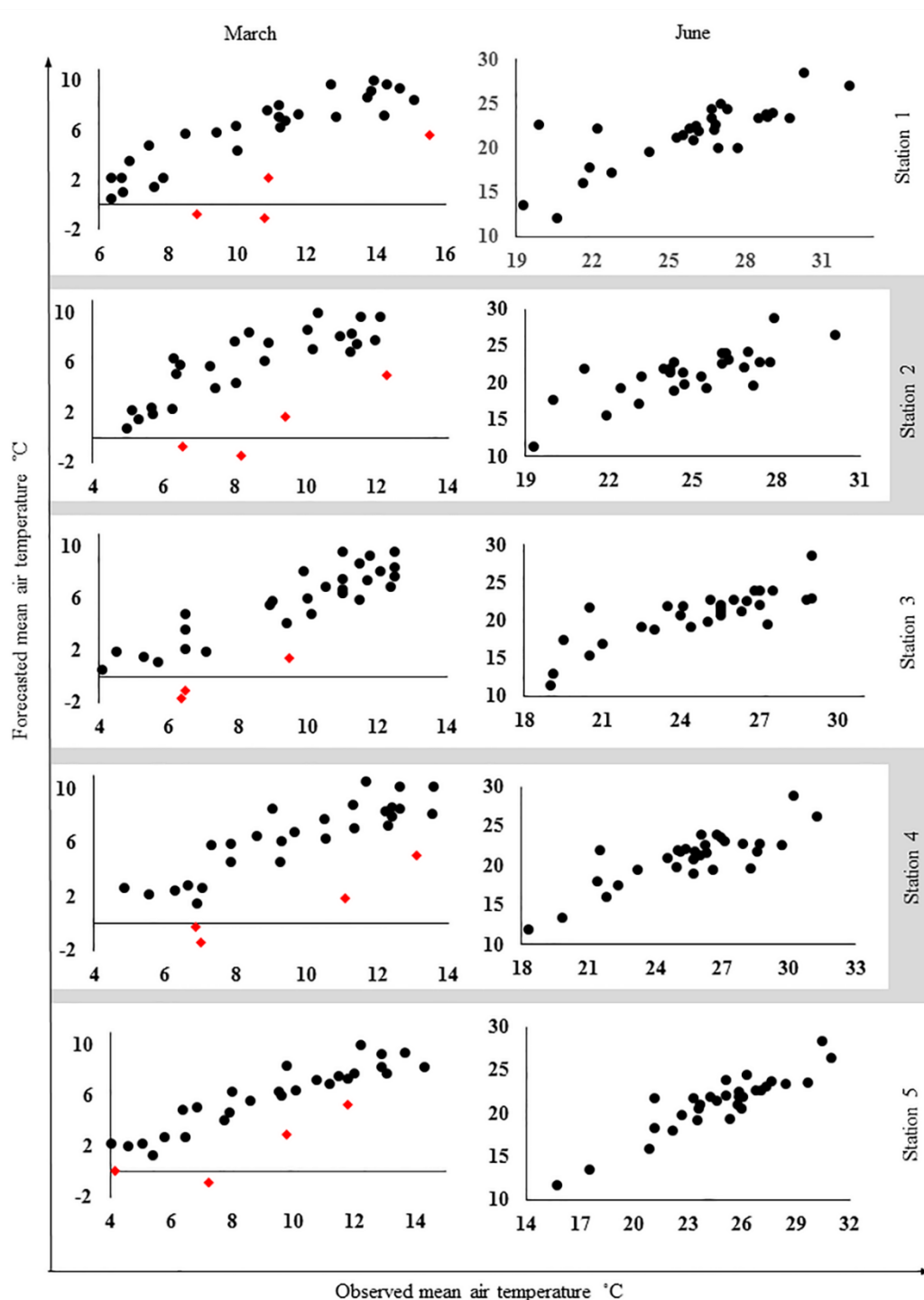


Figure 1: Study Area is located in Qazvin, Iran. This area covers the Qazvin irrigation network with total area of 3307 km<sup>2</sup> that is composed of agricultural fields, dominated by the growing of winter and summer crops, urban area, bare soil and natural vegetation. Weather stations are sparse and the minimum and maximum distance between stations are 13 and 78 km, respectively. For experimentation in this study, a sample subset of 3 × 8 grid points of ECMWF dataset is selected at 0.125° lat/lon distances.



**Figure 2:** Time series of the observed and the forecasted values at each station. The observed values are daily air temperature from weather stations and the forecasted values are daily air temperature from ECMWF at same locations. This figure shows the underestimation in ECMWF as well as spatial and temporal variability of bias.





**Figure 3:** Scatterplot of the observed and the forecasted values at each station. The observed values are daily air temperature from weather stations and the forecasted values are daily air temperature from ECMWF at same locations. Red points in the scatterplot denote the outliers.

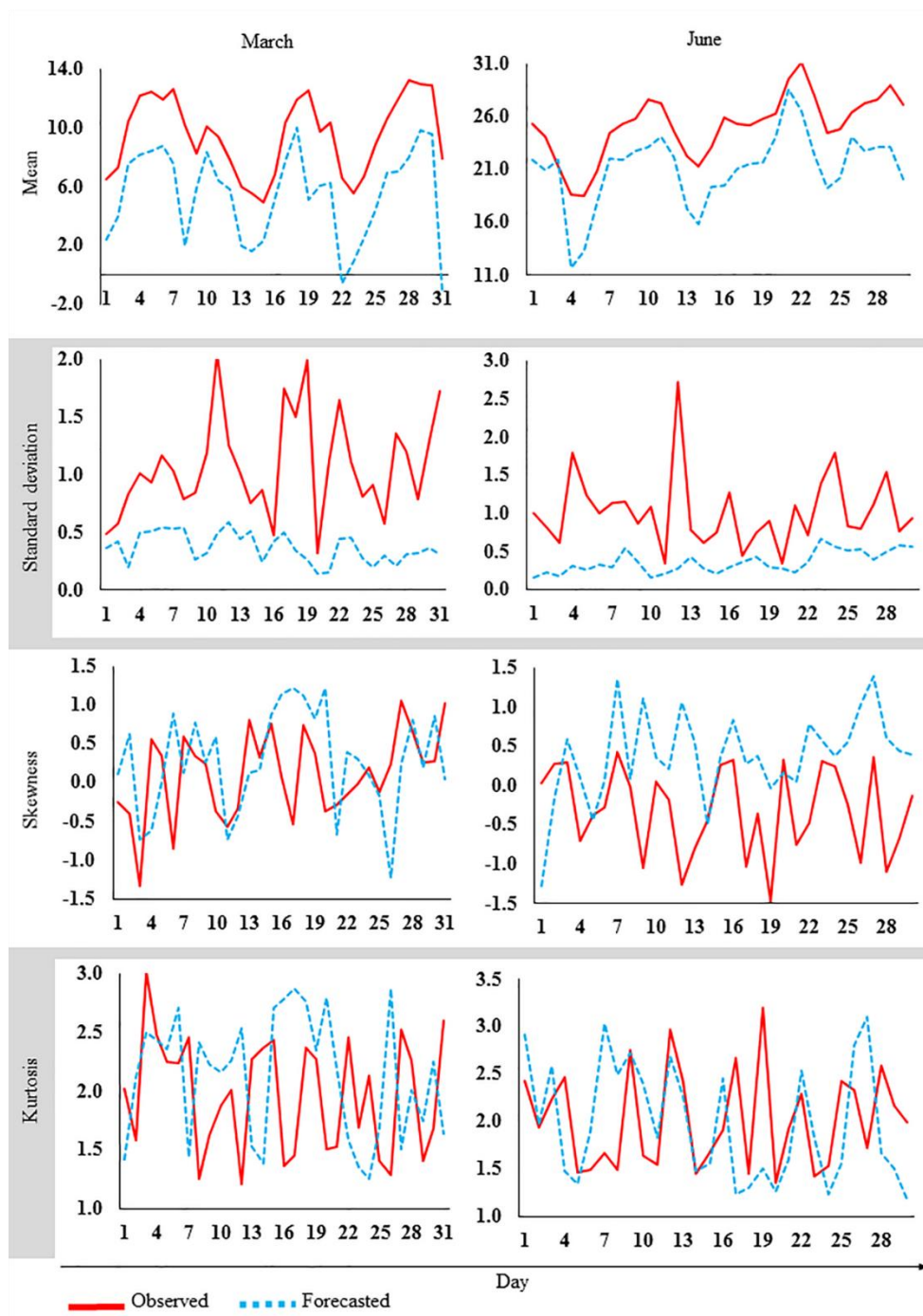


**Figure 4:** Bias between the moments of observed and forecasted marginals at each moment of time series. The observed values are daily air temperature from weather stations and the forecasted values are daily air temperature from ECMWF at same locations.

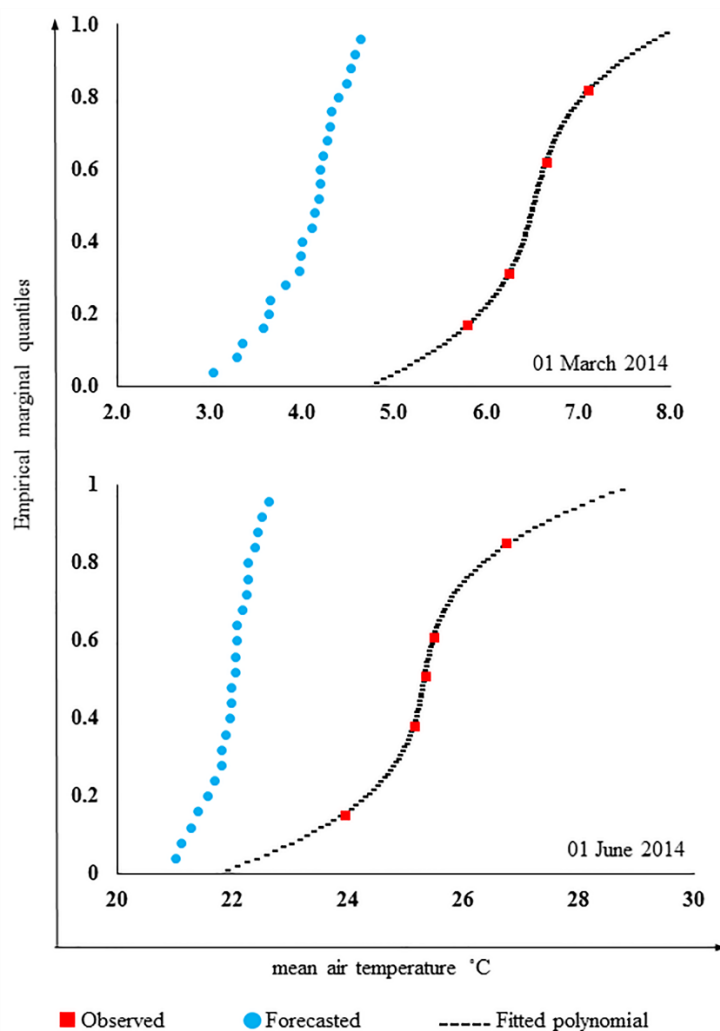


**Figure 5:** The empirical marginal values  $u_1$  and  $u_2$  and the fitted polynomial for observed and forecasted air temperature for first day of March and June.

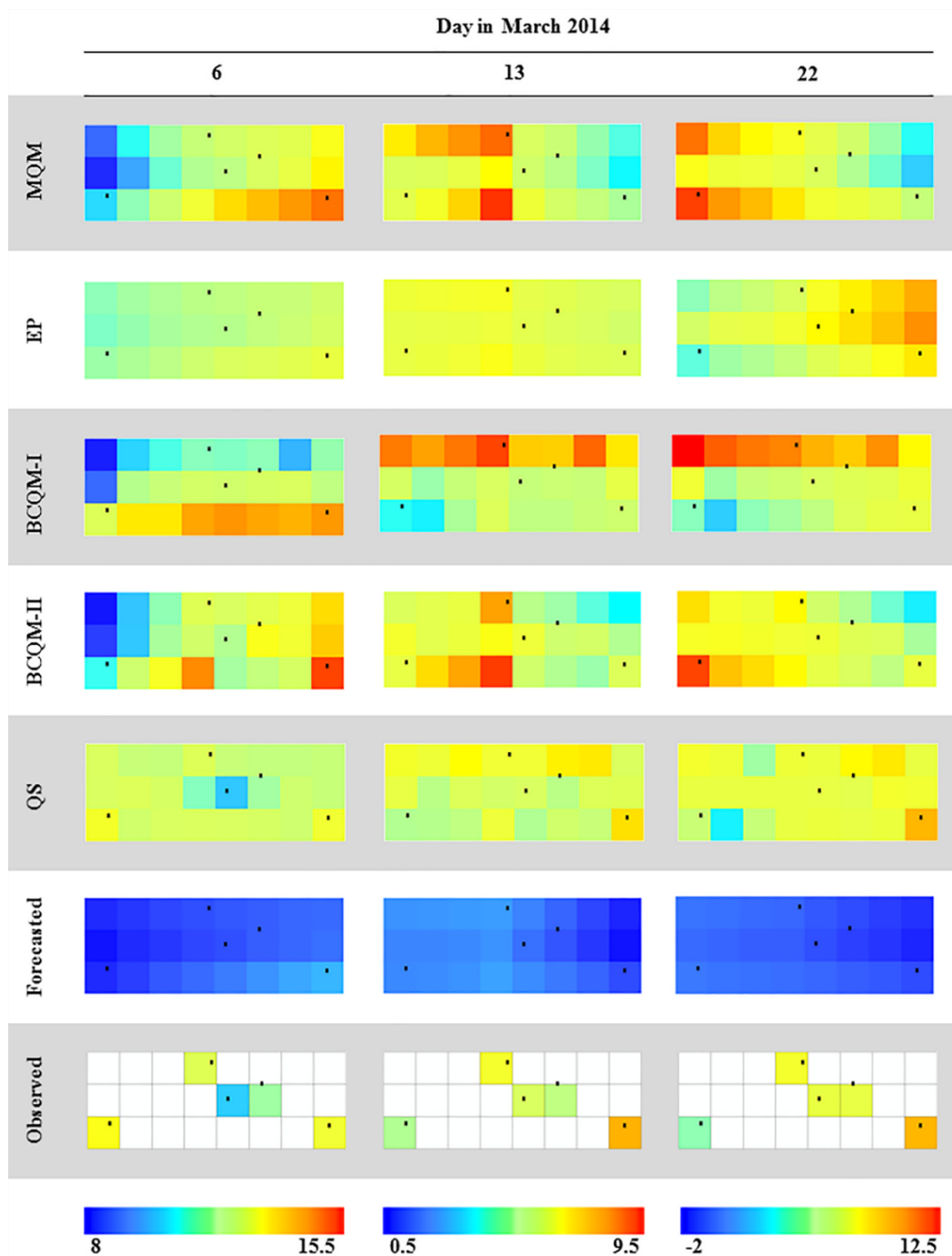


Figure 6: The spatial variability of the observed and the bias-corrected values comparing with the forecasted values over the study area in March 2014. The observed values are daily air temperature from five weather station, the bias-corrected values are the result of the bias correction methods and the forecast values are daily air temperature from ECMWF. For experimentation in this study, a sample subset of  $3 \times 8$  grid points of ECMWF dataset is selected at  $0.125^\circ$  lat/lon distances.

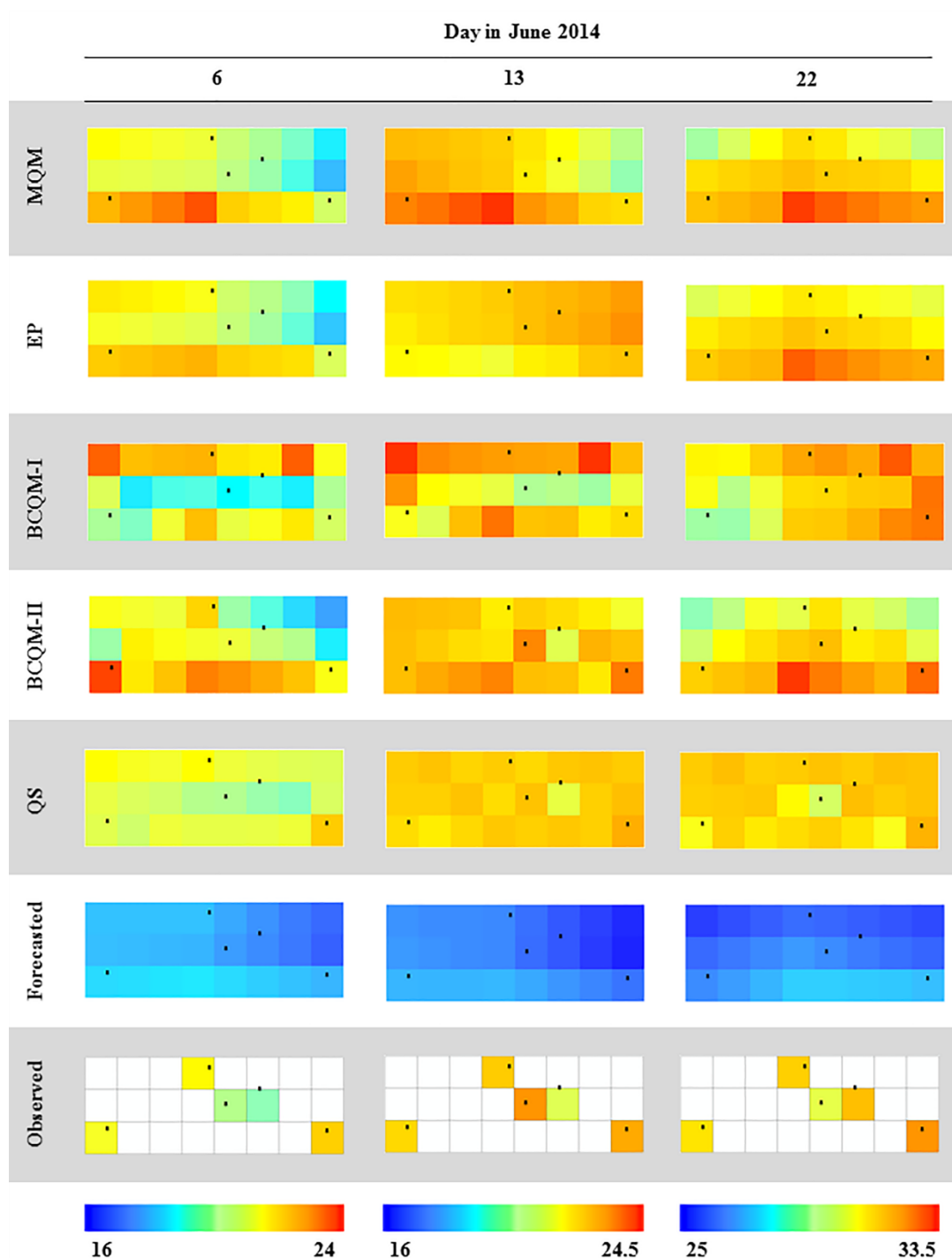


Figure 7: The spatial variability of the observed and the bias-corrected values comparing with the forecasted values over the study area in June 2014. The observed values are daily air temperature from five weather station, the bias-corrected values are the result of the bias correction procedures and the forecasted values are daily air temperature from ECMWF. For experimentation in this study, a sample subset of  $3 \times 8$  grid points of ECMWF dataset is selected at  $0.125^\circ$  lat/lon distances.